

## Fast Sampling, Rapid Filtration Apparatus: Principal Characteristics and Validation from Studies of D-Glucose Transport in Human Jejunal Brush-Border Membrane Vesicles

Alfred Berteloot, Christiane Malo, Sylvie Breton, and Michel Brunette

Membrane Transport Research Group, Department of Physiology, Faculty of Medicine, University of Montréal, Montréal, Québec, Canada, H3C 3J7

**Summary.** Kinetic data in (brush-border) membrane vesicles which rely on the validity of the initial rate assumption for their interpretation and depend on tracer flux studies using the rapid filtration technique for their experimental measurement have been limited to some extent by the absence of techniques that would allow for real-time data analysis. In this paper, we report on our successful design of a fast sampling, rapid filtration apparatus (FSRFA) which seems to fill up this technical gap since showing the following characteristics: (i) rapid injection (5 msec) and mixing (less than 100 msec) of small amounts of vesicles (10–40  $\mu$ l) with an incubation medium (0.2–1.0 ml); (ii) fast (20 to 80 msec depending on the sample volume) and multiple (up to 18 samples at a maximal rate of 4/sec) sampling of the uptake mixture followed by rapid quenching in the stop solution (approximately 5 msec) according to a predetermined time schedule (any time combination from 0.25 to 9999 sec); and (iii) fast, automated, and sampling-synchronized filtration and washings of the quenched uptake medium (only 15–20 sec are necessary for the first filtration followed by two washings and extra filtrations). As demonstrated using adult human jejunal brush-border membrane vesicles and Na<sup>+</sup>-D-glucose cotransport as models, the FSRFA accurately reproduces the manual aspects of the rapid filtration technique while allowing for very precise initial rate determinations. Moreover, the FSRFA has also been designed to provide as much versatility as possible and, in its present version, allows for a very precise control of the incubation temperature and also permits a few efflux protocols to be performed. Finally, its modular design, which separates the fast sampling unit from the rapid filtration device, should help in extending its use to fields other than transport measurement.

**Key Words** multiple sampling · fast quenching · rapid filtration · rapid kinetics · membrane vesicles (human intestine) · Na<sup>+</sup>-glucose cotransport

### I. Introduction

Kinetic studies that rely on initial rate measurements, when applied to ion or metabolite fluxes through artificial or biological membranes and to

enzyme reactions in membrane or immobilized systems, often have to overcome a rather challenging methodological problem since most of these processes have been shown to maintain their true initial rate conditions for not more than a few seconds at best. More specifically, (co)transport phenomena in (brush-border) membrane vesicles are fast processes due to an unfavorable surface/volume ratio of the vesicles as compared, for example, to isolated cells or intact tissues. As such, these lead very rapidly to either significant substrate accumulation into, or substrate depletion from, the intravesicular space during influx or efflux experiments, respectively. The situation is still worse under the so-called “zero-trans gradient conditions” often used to study the Na<sup>+</sup>-cotransport systems of the intestinal and renal epithelial cells using isolated brush-border membrane vesicles. In this case, since gradients for both the driving ion and the driven substrate are present at the start of an experiment, early collapse of the chemical gradients for ion and substrate might also be accompanied by membrane potential changes. Obviously, rapid modifications in the initial conditions might impair seriously any attempt at a kinetic characterization of such systems if true initial rates cannot be evaluated under a set of different conditions used for an experiment. Such problems have already been discussed at length in a few recent reviews and the reader is referred to these for more complete information [1, 4, 18, 22, 23, 27, 29].

Up to now, tracer flux measurements in vesicle studies have been made according to the so-called “rapid filtration technique” [15] which basically involves the three following steps [29]: (i) mixing of the vesicles with an incubation medium containing a radioactive substrate and other constituents as re-

quired; (ii) stopping of the reaction at established time intervals in a so-called "stop solution," often containing a specific inhibitor of the transport system under study; and (iii) filtration and washing of the resulting mixture in order to wash out the non-transported, radioactive substrate. The filters can then be recuperated and counted in order to determine substrate uptake. In principle, efflux studies can also be carried out following a similar protocol using vesicles preloaded with a radioactive substrate. Obviously, each of these steps is associated with a number of problems which have been extensively discussed previously [4, 18, 22, 23, 27, 29] and alternative methods have been proposed to circumvent some of these [7, 12, 25, 28].

Actually, the most critical limitations of the rapid filtration technique appear to be those associated with the rapid mixing of the vesicles and the incubation medium (which deals with the reliability of the zero time), the sampling over short time periods (which makes it difficult to measure true initial rates of transport), and the duration of the stopping process (which may be accompanied by leak of substrate out of the vesicles). Most of these are particularly relevant when using the manual version of the procedure, and two different types of apparatus have already been designed in order to overcome these limitations. The first one [16] is a semiautomatic mixing/diluting device which automatizes both the mixing of the vesicles with the incubation medium and the stopping of the reaction but not the filtration process. Such a machine allows for short incubation times in the range of 0.5 to 5 sec using 10 to 20  $\mu$ l of vesicle suspension and incubation medium. As noted by the authors, this instrument can only give an accurate time for the start and the stop pulse, while the actual time of incubation is certainly different due to time delays during the stopping process (40–60 msec) and initial complete mixing (approx. 70 msec). Such errors might limit the precision of the measurements over the shortest time points but do represent a significant improvement as compared to the manual approach. The second apparatus [10] is a rapid filtration system for membrane fragments or immobilized enzymes which couples the time-controlled incubation with a filtration step and allows for time resolutions in the order of 10 to 20 msec in the best cases. However, the filter is not washed at the end of the incubation period, thus limiting this technique to efflux studies or to very active preparations for influx studies. Moreover, since a continuous flow of radioactive substrate has to be maintained during the incubation process, such a technique might become prohibitively expensive for long incubation periods during influx measurements. This apparatus has been successfully used with some membrane preparations [8] but, to our

knowledge, has not yet been applied to brush-border membrane vesicle studies. It should finally be noted that automated techniques have also been proposed for efflux studies [11, 13] but, again, that they do not seem to have ever been applied to brush-border membrane vesicles.

A final aspect of flux measurements into membrane vesicles needs to be considered and concerns the complexity of the uptake measurement itself which includes both specific and nonspecific components which are: (i) the background radioactivity which is constituted by nonspecific and nonsaturable trapping of radioactive substrate in a dead space, likely representing radioactivity bound onto the filters and/or trapped in the water space surrounding the vesicles and filling leaky vesicles; (ii) the simple (passive) diffusion of substrate which represents the intrinsic leak permeability of the membranes to different substrates; (iii) the nonspecific and/or specific binding of substrate to intra- and/or extravesicular membrane sites; and (iv) the carrier-mediated process(es) which can be of either the facilitated or secondary active types and actually represent(s) the system(s) that one typically wants to study. Obviously, all of these components in uptake measurements need to be evaluated and separated for meaningful transport kinetic analysis to be obtained. As previously discussed by Dorando and Crane [9] and recently analyzed by Berteloot and Semenza [4], it clearly appears that some of these components would be easier to differentiate from each other (particularly as to components *i–iii* above) by analyzing real-time data, that is by considering uptake time courses obtained by aliquoting samples of vesicles from the same incubation medium at different time intervals. Moreover, since there is recent evidence for early deviations from linearity in uptake time courses [3, 24] compatible with the observation of presteady-state kinetics [24, 30], it clearly appears timely to develop a new apparatus that would permit the analysis of such phenomena.

During the last three years, our laboratory has devoted much effort in building an apparatus that would allow for measurements of real-time data in flux measurements, thus avoiding the limits of the one time point approach which is the lot of the two existing machines described above. During our successive trials, we paid much attention to resolving the following problems: (i) fast mixing of vesicles and incubation medium to initiate the reaction; (ii) fast and multi-sampling of aliquots from the same incubation medium; and (iii) fast filtration and washing of the recuperated samples. Obviously, care was also taken to get as much versatility and reproducibility as possible in this apparatus. As such, we included precise control of temperature and sampling volume as well as the possibility for efflux

measurements. In this paper, we report our success in constructing such a machine which we now call the fast sampling, rapid filtration apparatus (FSRFA). We thus describe the main characteristics of this apparatus and present most of the controls which were performed to validate this new technique. We also demonstrate, using human intestinal brush-border membrane vesicles and  $\text{Na}^+$ -D-glucose cotransport as models, that our machine compares favorably with the manual rapid filtration technique. Finally, in the accompanying paper [21], we report on the improvements that might be expected from using the dynamic approach allowed by the FSRFA and on the new insights as to the meaning of kinetic data that the use of this technique has brought to our attention.

## II. Materials and Methods

### A. CHEMICALS

All salts and chemicals for buffer preparation were of the highest purity available. D-(1-*n*-<sup>3</sup>H)mannitol (19.1 Ci/mmol) was purchased from New England Nuclear and D-(U-<sup>14</sup>C)glucose (315 mCi/mmol) from Amersham Canada Limited. Pyranine was purchased from Molecular Probe, and amiloride hydrochloride was a gift from Merck, Sharp and Dohme Canada, Division of the Merck Frosst Canada, Kirkland, Quebec. Phlorizin was purchased from Aldrich Chemical.

### B. MATERIALS

The main components of the apparatus and their respective suppliers are as follows: recirculating water bath (Lauda, Brinkman); thermoprobe (Yellow Spring Instrument); regulator (American Standard); manometer (USG); Venturi (CompAir Tools & Controls); impulsion valve (Skinner Electric Valves); pressure valve (Swagelock); other valves (General Valves); stepping motor (Applied Motion Products); vacuum pump,  $\frac{1}{2}$  HP, 1725 rpm, 29 inches of mercury pressure (AC Motor, Emerson Electric Canada); Teflon-O-rings (National O-Rings); polyethylene tubings (PE-90, Clay Adams); and disposable pipette tips (American SMI).

### C. PREPARATION OF BRUSH-BORDER MEMBRANE VESICLES

Adult human small intestines were obtained from healthy organ donors with the kind collaboration of Drs. J. Cardinal and J. Corman from Maisonneuve-Rosemont and Notre Dame Hospitals, respectively. The jejunum was collected, flushed with ice-cold 0.9% NaCl, cut into 20-cm long pieces and frozen at  $-80^{\circ}\text{C}$  until further processing. The  $P_2$  fractions were prepared as follows: the jejunum sections were thawed and the mucosa was scraped with a spatula on a cold glass plate. Brush-border membranes were purified by the calcium chloride precipitation method of Schmitz et al. [26], and vesicles were obtained according to Hopfer et al. [15] with the following modifications:  $P_3$  fractions were resuspended in a solution containing 50 mM Tris-HEPES

buffer (pH 7.5), 0.1 mM  $\text{MgSO}_4$ , 250 mM KCl, and a cocktail of protease inhibitors (pepstatin 0.01 mg/ml, chymostatin 0.01 mg/ml, aprotinin 1.25  $\mu\text{g}/\text{ml}$  and bacitracin 0.1 mg/ml) to a final concentration of 10 mg protein/ml and were frozen in liquid nitrogen. On the day of the experiment, a number of  $P_3$  fractions were thawed and the vesicles were prepared as a  $P_4$  fraction as described previously [2, 3]. This procedure allows for the preparation of a large amount of vesicles from the same batch without any loss in transport activity. Based on sucrase activity, enrichment factors in the range of 8- to 12-fold over the mucosal homogenate were routinely obtained.

### D. ASSAYS

Sucrase (EC 3.2.1.48), a marker enzyme for the brush-border membrane, was routinely assayed by measuring glucose liberated as described by Kunst, Draeger and Ziegenhorn [17]. The protein content was determined using the BCA Protein Assay Reagent (Pierce Chemical) with bovine serum albumin as standard.

### E. TRANSPORT STUDIES

Uptake studies were performed using a manual rapid filtration technique as previously described [2, 3, 20] or our newly designed FSRFA as discussed in Results. The exact composition of the resuspension buffer for brush-border membrane vesicles as well as the final concentrations in the incubation media are indicated in the legends to the figures. Amiloride was included in all transport experiments at a concentration of 0.5 mM to inhibit the  $\text{Na}^+/\text{H}^+$  exchanger [3]. As described previously for the manual procedure [2, 3], 50- $\mu\text{l}$  aliquots were taken at time intervals from the incubation mixture, poured in 1 ml quenched ice-cold stop solution, filtered on prewetted 0.65- $\mu\text{m}$  (Micro Filtration System) or 0.45- $\mu\text{m}$  (Sartorius SM 11306) cellulose nitrate filters and washed with 4 ml nonradioactive ice-cold stop solution. Filters were dissolved in minivials with 5 ml Filter Count (United Technologies Packard) [3]. <sup>3</sup>H and <sup>14</sup>C radioactivities were determined using a Minaxi Tri-Carb, Series 4000, model 4450 scintillation counter (United Technologies Packard).

Results are expressed as nmol solute uptake  $\cdot$  mg protein<sup>-1</sup>. Initial rates of transport, estimated by linear-regression analysis over the linear part of the uptake-time curves, are expressed as pmol solute uptake  $\cdot$  sec<sup>-1</sup>  $\cdot$  mg protein<sup>-1</sup>. Regression analysis was performed using an Apple IIe microcomputer and a curve fitter program (P.K. Warme, Copyright ©, 1980, Interactive Microwave). Statistical analyses were done with Statcalc (A. Lee, P. McInerney, and P. Mullin, Copyright ©, 1984) using the same microcomputer.

## III. Results

### A. DESCRIPTION AND MAIN CHARACTERISTICS OF THE FAST SAMPLING, RAPID FILTRATION APPARATUS (FSRFA)

#### 1. Overview of the FSRFA and Its Functioning

A photograph of the FSRFA and its working parts is shown in Fig. 1. The main parts of the apparatus consist of a vesicle injector (A) which is mounted on

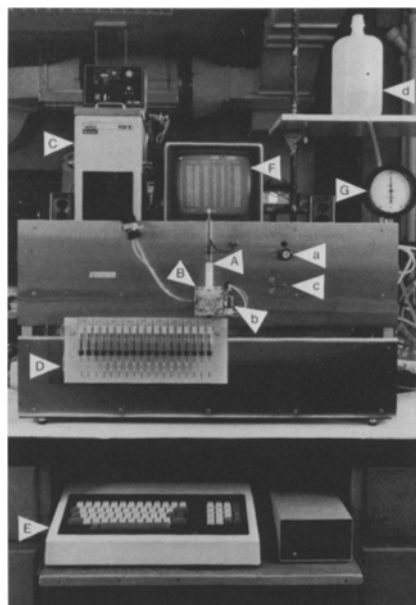


**Fig. 1.** Photograph of the fast sampling, rapid filtration apparatus, (FSRFA). The main features of this system are: (A) vesicle injector; (B) incubation chamber with loading control (a), washing valve (b) and washing switches (c); (C) recirculating water bath connected to the chamber; (D) manifold array connected to stop solution bottle (d) for washings; (E) microcomputer and keyboard; (F) monitor for visual control of the parameters; and (G) air pressure control. Details on the general functioning are given in the text

top of an incubation chamber (B) thermoregulated through a connection with a recirculating water bath (C). Vesicles can be loaded easily into the injector which is simply screwed to the incubation chamber (see section 2 below). A gentle suction controlled by valve (a) (see section 3 below) allows the loading of the incubation medium into the incubation chamber through an opening in its bottom part. Samples are recovered in a manifold array (D) made of 18 individual filter holder units with their own system of filtering and washing (see section 5 below). The filters are easily loaded and unloaded from their respective holders since both up (working) and down (resting) positions are available. The stop solution (in general 1 ml) contained in bottle (d) (usually kept on ice) can be automatically delivered to the upper chamber of the filter holder units such as to be ready to receive the vesicle samples and efficiently and rapidly stop the reaction. The manifold array (D) shuttles below the incubation chamber according to a predetermined time sequence and allows for fast sample recuperation. During the washing and filtering procedures, a predetermined sequence of filling the upper chamber with stop solution and filtering is performed. At the end of a run, the chamber can be

semiautomatically washed out with deionized water (container not shown on Fig. 1) using valve (b) and switches (c) (see section 4 below).

The inside of the main body of the apparatus contains all the valves, manifolds, tubings, and electronics which compose the different circuits involved in the control of the functioning of the chamber and the manifold array (see sections 3 through 5 below). It also contains a homemade microcomputer which controls the synchronization of the sequences required for injection, mixing, sampling, washing, and filtering. This computer is connected to a standard microcomputer (E) which allows for easy communication between the experimenter and the machine. Actually, all of the parameters which can be modified are easily keyed in computer (E) and visualized on monitor (F) (see section 6 below). To run the apparatus, all that is needed is an air pressure system (the working pressure being controlled by manometer (G)), a vacuum pump, and, of course, electricity.

## 2. Vesicle Injector and Incubation Chamber

A magnified view of the vesicle injector mounted on top of the incubation chamber (Fig. 1, parts A and B) is shown on Fig. 2. As can be viewed from that figure, the injector *per se* is composed of a plastic bottom part which just serves as a pipette holder and can be screwed in and out of the incubation chamber. The upper part of the vesicle injector screwed on the plastic bottom part, contains a homemade, spring-activated piston system which is manually compressed and held in this position by pin (A). Injection of the vesicles starts by manually removing pin (A). The whole sequence of mixing, sampling, filtration and washing is then triggered by an electric signal (B) which is activated along the down run of the piston and sent to the machine microcomputer. This device allows for a very precise recording of the zero time. A direct estimate of the time required for the injection was performed using two electrodes, one in the chamber and the other one sensing the signal of the piston. It was thus found that not more than 5 msec are required for this step.

The incubation chamber is made of plexiglass and is mounted on a hollow brass block which is connected through tubing (C) (see Fig. 2) to a recirculating water bath (Fig. 1, part C). This allows for temperature control of the transport reaction from 5 to 45°C. Since the heat exchange between brass and plastic is not particularly good and since the water bath is not very close to the incubation chamber, the real temperature of the reaction mixture had to be monitored from the inside of the chamber, by using

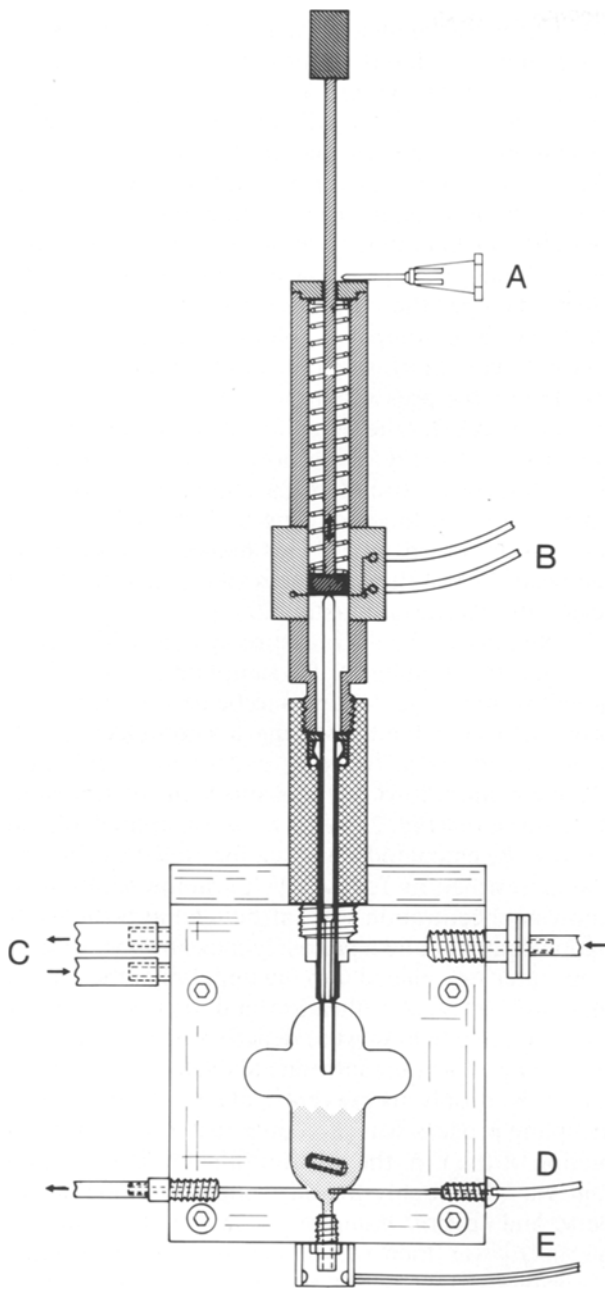


**Fig. 2.** Vesicle injector and incubation chamber. The main components are as follows: (A) pin controlling the injection of vesicles inside the chamber; (B) electric signal activated during vesicle injection and controlling the start of all automated sequences; (C) thermoregulation circuit of the chamber in connection with a recirculating water bath; (D) thermoprobe which provides continuous reading of the incubation temperature; and (E) photoelectric cell sensing the sampled drops and measuring the sampling time. Details on these different components are given in the text

a thermoprobe (Fig. 2, D). This thermoprobe was calibrated against a range of precisely determined temperatures, and the standard curve was introduced into the computer. Since the thermoprobe

is permanently coupled to the two computers, the temperature in °C can be read at any time from the monitor (Fig. 1, part F).

As can be seen from Fig. 2, we had to specifically design the inside shape of the incubation chamber. As will be discussed later, the functioning of the chamber relies on an alternation between inside negative and positive pressures such as to allow for fast sampling. Moreover, in the earlier versions of the chamber, continuous bubbling had to be maintained to keep the incubation mixture from leaking out which resulted in considerable foaming with the formation of very big bubbles that could not burst in a round-shaped chamber and would contaminate the air circuit. Hence, a cruciform design which allows for bubbling without those problems was elaborated. It should be noted that bubbling has now been reduced to a minimum (*see below*), but that this shape is still very convenient since it serves to increase the inside air volume. As such, liquid is restricted to the bottom part of the chamber with a maximum volume of 1 ml. This part also contains the magnetic stirrer (*see Fig. 2*) which is activated by a magnetic motor placed behind the chamber (not visible on Fig. 2). The magnetic stirrer is automatically activated from the start signal, and its action is automatically interrupted 100 msec following activation of signal (B) in order to minimize foaming of the vesicle suspension and any interference with the sampling sequence. It appears that complete mixing must occur during this time since initial linearities in uptakes are always observed (*see below*). It should be noted in this context that this step does not appear crucial since a very small volume of vesicles (10 to 40  $\mu$ l) is forcibly injected into a much larger volume (0.25 to 1 ml) and thus, by itself, the injection already allows for a good dispersion of the vesicles into the incubation medium.

### 3. Air Pressure and Vacuum System Controlling the Functioning of the Incubation Chamber

It should be noted from Fig. 2 that the chamber is permanently open to the exterior through a small needle screwed in its bottom part. Such a system was found most useful since it avoided the necessity for the in and out control of liquid flow through any kind of valve or mobile systems, our early attempts with these having proved very frustrating. In these conditions, it is thus obvious that we had to design a special system that would allow for liquid retention inside the chamber while allowing for fast sampling of aliquots, a problem which was solved by using the air pressure/vacuum system to be now described. The upper part of the incubation chamber

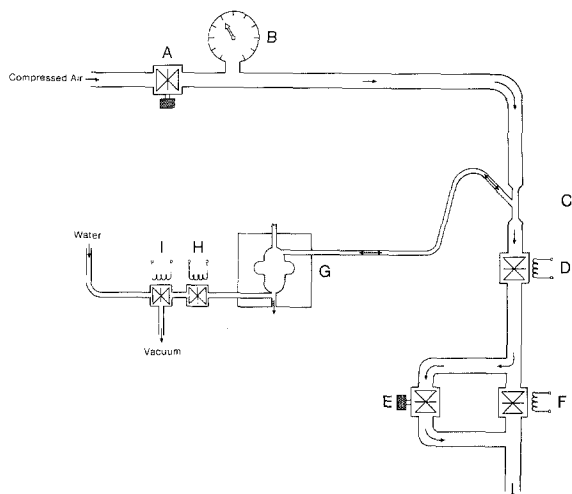


**Fig. 3.** Air pressure and vacuum system controlling the functioning of the incubation chamber. Air pressure from a table outlet can be controlled through regulator (A) and manometer (B) and alimnts the main air circuit of the Venturi (C) (one-way arrows) while the side branch of the Venturi is connected to the incubation chamber (G). The vacuum so created in the chamber can be adjusted through valve (E) and reversed to positive pressure inside the chamber, which allows for fast sampling, and is controlled by impulsion valve (D). Valve (F) is then triggered to allow for prompt return of the negative pressure in the chamber. The semiautomatic washing circuit of the chamber is controlled by valves (H) and (I). More details are given in the text

is connected to an air pressure system (Fig. 2, arrow at upper right) which controls both the loading of the incubation medium into the chamber and the sampling of aliquots from the vesicle mixture into the manifold array. This circuit is shown in Fig. 3 where the incubation chamber has been schematized as (G). The chamber is directly connected to a Venturi (from the name of the inventor, Y-shaped tubing (C) in Fig. 3) in which compressed air (10 to 40 psi) is allowed to flow under the control of a regulator (A) connected to manometer (B) (which corresponds to (G) in Fig. 1). When flowing in the principal circuit (one way arrows in Fig. 3), the compressed air establishes a vacuum in the branch of the Venturi which is connected to the chamber (double arrows in Fig. 3). Thus control of air flow through valve (E) in Fig. 3 (corresponding to valve (a) in Fig. 1) allows for control of the negative pressure inside the chamber. Loading of the incubation medium inside the chamber can thus be performed with valve (E) open which increases the vacuum in the chamber. The incubation medium of desired composition and preset volume (from 0.25 to 1 ml) can thus be aspirated inside the chamber in a quantitative way using a small polyethylene tubing inserted on the bottom opening of the chamber. Valve (E) is then turned down such

as to keep the minimum negative pressure inside the chamber which is necessary for preventing the medium from falling out. The sensitivity of the system is now such that constant bubbling is not necessary anymore for performing this task.

The same circuit is also used for sampling from the incubation chamber since blocking the air flow in the principal circuit by impulsion valve (D) transforms the negative pressure inside the chamber into a positive one, thus forcing some liquid out of the chamber. The sampling volume can therefore be controlled by the closing time of the impulsion valve (D) and by the pressure applied to the main circuit. Immediately after the reopening of valve (D), impulsion valve (F) (Fig. 3) is now triggered and fully opens the main circuit for a short predetermined time (10 msec), thus allowing for a maximum vacuum inside the chamber. This maneuver minimizes the dead time of the apparatus since the circuit can regain its initial state faster.

Obviously, the air pressure system which controls the functioning of the sampling process does not allow for preset volumes to be determined. This problem was solved by using a photoelectric cell which is placed at the very exit of the incubation chamber and allows for measurement of the sampling duration (Fig. 2, part E). The sampling volume can now be estimated from a calibration curve which was performed as follows. A pyranine solution of known concentration was introduced into the incubation chamber and a precisely measured volume of 1 ml water was placed into the upper chamber of the manifold array. All filtration and washing circuits (*see* section 5 below) were deactivated so that, with this set up, the filters introduced in each filter holder unit served only to prevent leakage of liquid. The sampling process was then initiated and, after completion of the run, the content of each recuperation unit was thoroughly mixed using an automatic pipette and several pumping in and out. An aliquot of 900  $\mu$ l was then manually extracted from each reservoir, and the pyranine concentration measured in a spectrophotometer at a wavelength of 454 nm. The resulting calibration curve, as obtained using different pressures (15 to 25 psi) in the main air circuit and different closing times (12 to 30 msec) for valve (D) of Fig. 3, is shown in Fig. 4 (filled symbols). These results demonstrate a very good linear relationship ( $r = 0.991$ ) between the sampling volume (15 to 90  $\mu$ l) and the sampling duration (20 to 80 msec) under all sets of conditions. Extrapolation of this straight line to the time axis shows an intercept of 11 msec which actually corresponds to the minimum time required to go from inside-negative to inside-positive pressure in the chamber after closing of valve (D) in Fig. 3 and thus represents the inertia

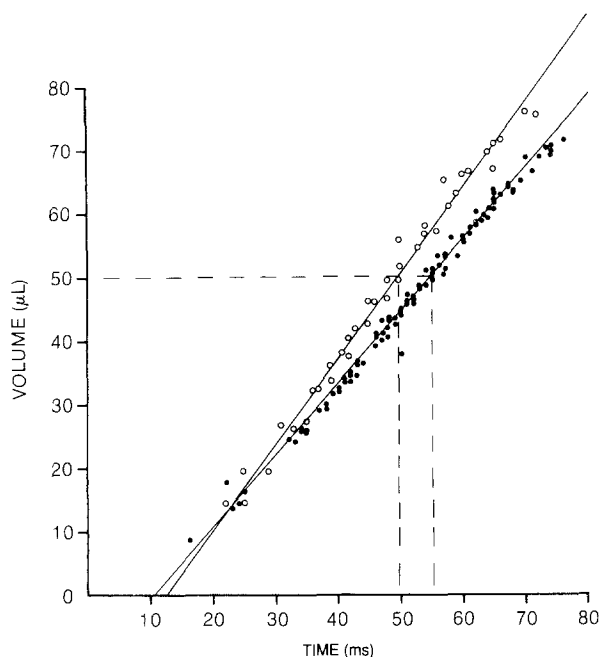


**Fig. 4.** Relationship between the sampling time and the sampling volume in the absence (●) and presence (○) of membrane vesicles. The sampling volume, measured with pyranine as described in the text, was estimated at different pressures (15 to 25 psi) and different impulsion times (12 to 30 msec) while the sampling time was estimated from the photoelectric signal. The lines shown were obtained by linear regression over the data points. A 50- $\mu$ L volume is obtained for sampling times of 50 or 55 msec at 15 psi and 18 msec impulsion time in the presence and absence of vesicles, respectively. Full details are given in the text

of the air pressure system. Similar results were obtained using a mixture of membrane vesicles and pyranine inside the incubation chamber (Fig. 4, open symbols). In that case, the extrapolated intercept on the time axis (12.5 msec) of the linear relationship ( $r = 0.993$ ) is entirely compatible with the dead time determined in the absence of vesicles. However, a slight increase in the slope value as compared to the situation in the absence of vesicles was found, a quite logical finding when considering the difference in medium viscosity between these two situations.

Our working conditions in the presence of vesicles were thus set in the middle range of the time/volume relationship using 15 psi in the main air circuit and an 18-msec closing time for valve (D). Under these conditions, the reproducibility of the sampling process was estimated from the sampling durations on eight consecutive runs of 18 samples each. The following mean sampling durations  $\pm$  SD (msec) were obtained:  $51.2 \pm 1.2$ ;  $51.9 \pm 1.3$ ;  $50.7 \pm 1.6$ ;  $52.4 \pm 2.1$ ;  $52.5 \pm 1.6$ ;  $51.3 \pm 1.1$ ;  $51.4 \pm 1.7$ ; and  $52.4 \pm 1.5$ . It thus appears that the SD of these

measurements represent a 2.1–4.0% variation around the mean value on a run of 18 samples. However, since the range of variation between the lowest and highest values during single or consecutive runs (49–56 msec in the above measurements) can represent as much as 10–15% of these mean values, the sampling duration times are routinely monitored in our experiments and standardized to a duration time of 50 msec which corresponds to a 50- $\mu$ L sampling volume according to the curve shown in Fig. 3.

It is thus clear that such a system allows for fast, multiple, and reproducible sampling from the same mixture with a very small dead time which is actually fixed by the sampling duration (volume). From the above numbers, it can be readily seen that the injection system could operate at a rate of 10 samples per sec with a 50- $\mu$ L sampling volume.

#### 4. Washing Circuit of the Chamber

A semiautomatic washing circuit is also connected to the bottom of the chamber (lower left arrow in Fig. 2) and is presented on the left side of Fig. 3. When the valve (H) is closed, this circuit is not connected with the incubation chamber and the three-way valve (I) (corresponding to valve (b) in Fig. 1) is opened to the vacuum circuit which is under the control of the vacuum pump. The residual medium present in the incubation chamber is aspirated by this vacuum circuit after opening of the valve (H) by manual control of the left switch (c) of Fig. 1. Inversing the position of the right switch now opens the valve (I) of Fig. 3 to a flow of deionized water which fills up the chamber by gravity. This sequence can be repeated, and a minimum of five consecutive washings were found necessary to properly clean the chamber between assays as estimated from radioactivity measurements after consecutive washings.

#### 5. Functioning of the Filter Holder System and Manifold Array

The manifold array (Fig. 1, part D) is formed by a movable plexiglass block on which are fixed 18 filter holder units. The plexiglass block is fixed on an endless rod which is firmly attached to a stepping motor. Before each sampling, the motor steps forward to place one filter holder unit directly below the exit of the incubation chamber. The motor is controlled by the internal microcomputer of the apparatus and so, the sequence of sampling, filtration, and washings is fully automated and synchronized to a predetermined time sequence. Actually, it is the

functioning of this motor which sets the limit of the fast sampling sequence to 4 per sec.

Each filter holder unit is composed of an upper reservoir (1.5 ml) which allows for recuperation of the uptake mixture and to which is connected the washing circuit (*see below*). The lower part includes the filter holder *per se* which can move up and down such as to allow easy access for filter installation and removal between runs. An enlarged view of the top part of this filter holder system is shown on a scaled diagram at the upper right of Fig. 5. The filter support is screwed on a brass rod (*H*) which is connected to a syringe piston (Fig. 5, part *D*). The movement of the filter holder can thus be controlled through the movement of this syringe piston which is semiautomatically controlled through the holding circuit (*see below*). A lateral perforation in rod (*H*) also allows for connection of the filter holder to the filtering circuit (*see below*) through tubing (*I*). The filter support had to be specially designed as shown in the upper part of Fig. 5. A circular groove had to be engraved on the top of the Teflon filter support to maximize the filtering rate. Also, an air entry (*J*) had to be drilled through the Teflon support to ensure complete removal of liquid from below the filters and for drying out of the filters at the end of the last washing step. A Teflon O-ring (diagrammed on part *D* of Fig. 5) force-inserted into a groove at the bottom of the upper reservoir ensures a very good seal and prevents any loss of liquid during the filtering and the washing steps.

The three circuits ensuring the proper functioning of the filter holder units are also diagrammed in Fig. 5. The holding circuit, which is responsible for the *en bloc* up and down movement of the 18 filter holders, is shown at the bottom right of Fig. 5. This circuit is split into two parts by means of a three-way valve (*A*), one branch being connected to the 18 filter holders while the two other branches are connected to an air pressure supply and a vacuum pump, respectively. The air pressure is adjusted to 20 psi by means of a regulator (*B*) and a manometer (*C*). When connected to the air pressure system, the three-way valve allows for the air pressure to be applied on each filter holder piston and sets up the working, up position of the filters. At the end of a run, the vacuum circuit can be selected by triggering valve (*A*) to its other position, and each piston goes down because of the vacuum suction.

The filtering circuit (left bottom part of Fig. 5) is also connected to the same vacuum pump as above but is split into 18 individual lines through a manifold connected to 18 valves (*G*) such as to allow for independent control of the 18 filter units. Actually, different filtration times can be selected for each unit by controlling the opening time of valve (*G*).

Furthermore, this system also gives the flexibility to determine the number of washing sequences to be performed in each individual filter unit.

The washing circuit is diagrammed in the upper left of Fig. 5 and is alimented through connection to a bottle containing ice-cold stop solution and placed at a higher level than the apparatus (*see* Fig. 1). This solution is thus fed into the circuit by the sole force of gravity. Again, a manifold (*E*) connected to 18 valves (*F*) allows for splitting this circuit into 18 individual lines, and thus, for the washing of only one filter unit at a time. The volume of the washing solution to be delivered to each unit is controlled by the opening time of each valve. Obviously, the washing circuit is connected to the filtering circuit such as to allow for a coordinated sequence of filling and emptying.

As will be demonstrated later (section B.2. of Results), this system allows for rapid filtration and washings under conditions lasting just a few seconds. Also, the time required for the first drop of a sampled aliquot to reach the upper reservoir was found to be on the order of 5 msec or less.

## 6. Control of the Apparatus and Functioning Sequence

All parameters which can be controlled in the above circuits and all information pertinent to the functioning of the apparatus are shown on a picture of the monitor screen in Fig. 6. The first column identifies each of the 18 sampling units from right to left. The second column allows for the selection of a sampling sequence, and the number keyed in represents in sec each of the selected sampling times (any time combination from 0.25 to 9999 sec). The third column shows the sampling times in msec for each of the 18 samplings, and thus, allows one to standardize all samplings to the same volume from the calibration curve described above (*see* section 3) and shown in Fig. 4. The fourth column shows in msec the time selected for reversed pressure through the Venturi system while the fifth one indicates in msec the time selected for maximal vacuum following sampling as also described in section 3. The sixth column determines the number of washings in the individual filter units (number 3 means one filtration of the stopped sample plus two washings and filtrations). The last column allows for a delay sequence to be established in the filtration of the individual filter units and was included to allow for efflux studies to be performed (although these can only be done at room temperature since the filter units are not thermoregulated yet). The top line of the screen shows the temperature inside of the incubation chamber (*C*) as well as



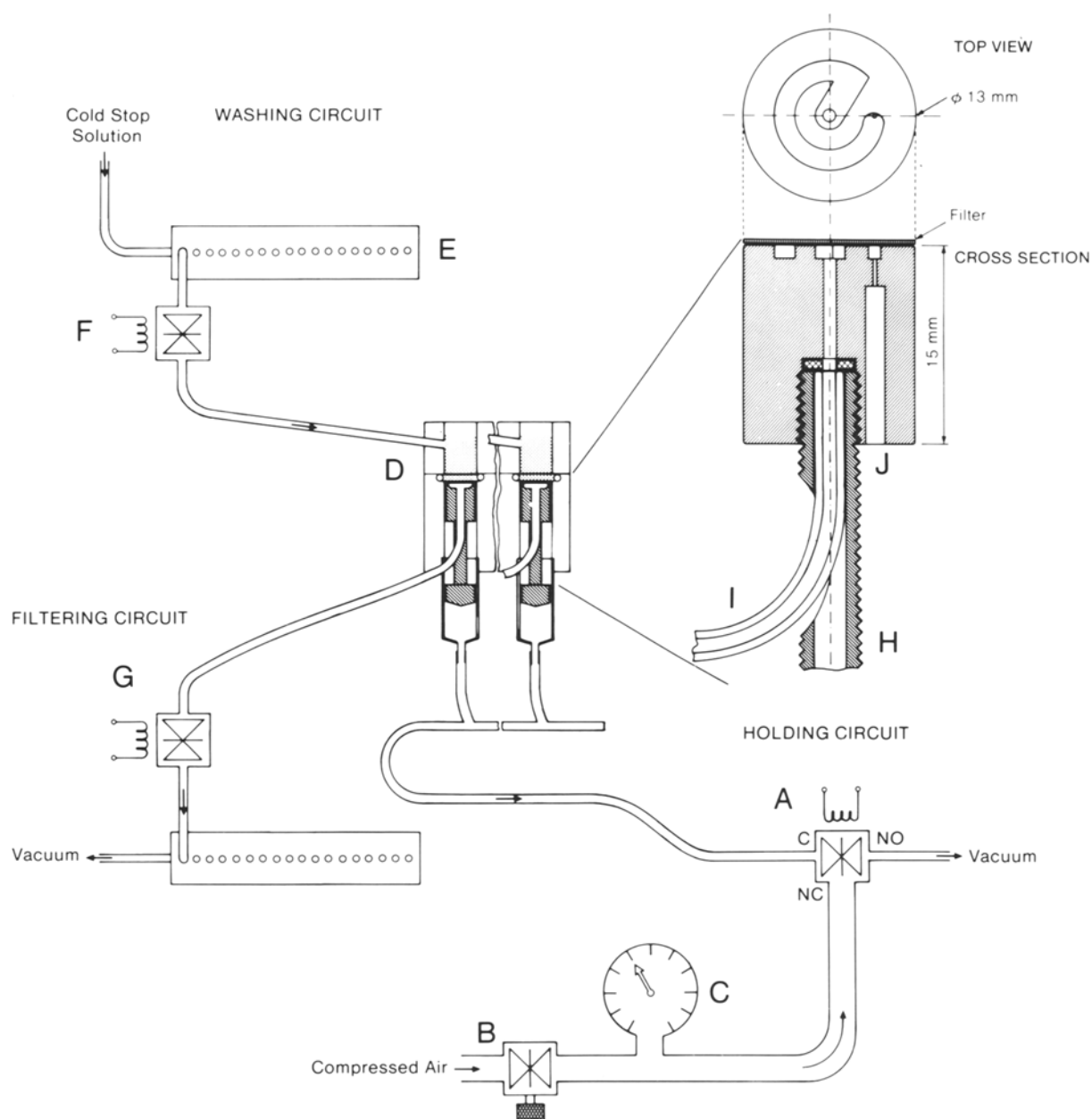


**Fig. 5.** Functioning of the filter holder system and manifold array. The manifold array (*D*) is composed of 18 filter holder units. The lower part of these units contains the filter holder *per se* (enlarged view shown on the scaled diagram) which can be moved up and down as controlled by the holding circuit. Filtration is controlled by the filtering circuit. The upper part of the filter holder unit is connected to the washing circuit which allows for multiple washings in synchronization with multiple filtrations. Full details of the functioning of the different parts are given in the text

the time elapsed from the start of an experiment (*T*). The bottom line of the screen allows for modification of both the filtration (*TF*) and washing (*TR*) times.

The following sequence is thus followed for a run to be complete: (i) Eighteen filters are set in place with forceps in each of the filter holder units, and the up position of these units is selected. (ii)

Five to 40  $\mu\text{l}$  of vesicles are manually loaded inside a pipette tip, and the vesicle-containing tip is introduced into the bottom part of the vesicle injector already screwed on top of the incubation chamber. The upper part of the vesicle injector is then screwed in its bottom part with the piston rearmed and maintained in its up position with the pin. (iii) The incuba-

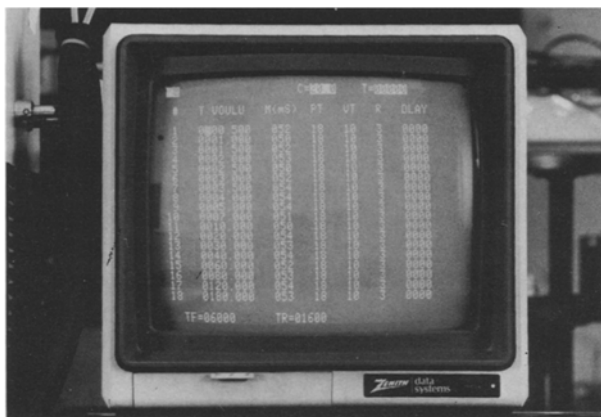


**Fig. 6.** Photograph of the control monitor showing the different parameters which are directly available for modification or real-time control. (C) inside chamber temperature; (T) total elapsed time from initiation of injection; (#) sample number; (T VOULU) time schedule for the different samplings; (M(ms)) measured sampling time through the photoelectric cell; (PT) impulsion time of the sampling valve; (VT) impulsion time for return to normal pressure; (R) number of washings per filter holder unit; (DELAY) delay in filtration after sampling in the individual filter holders units; (TF) filtration time; and (TR) filling time of the upper chambers of the filter holder units. Full details are given in the text

tion medium is aspirated inside the chamber. (iv) Ice-cold stop solution (1 ml) is automatically loaded into the upper chamber of each filter unit after keying in the order to the computer. (v) The start signal is keyed into the computer, which starts the magnetic stirrer (106 rpm). (vi) The pin is manually removed, and the piston allows for the injection of vesicles while triggering the whole sequence to follow. (vii) Mixing is stopped after 100 msec of injection, and the sampling sequence starts according to the predetermined time schedule. At the same time, filtration and washing start in those filter holder units which have already received a sample. (viii) At the end of the run, the filter holder units are set in the down position from the computer keyboard and the filters can be removed. The vesicle injector is removed, and the washing of the incubation chamber can be performed. With two persons working together to speed up the last two manual parts of this sequence, a run consisting of nine points over 4.5 sec can be performed every 5 min, approximately.

## B. APPLICATION OF THE FSRFA TO TRANSPORT STUDIES USING HUMAN INTESTINAL BRUSH-BORDER MEMBRANE VESICLES

### 1. Background Controls

Since the transport of organic molecules into (brush-border) membrane vesicles is often performed using a  $^{14}\text{C}$ -labeled substrate and a  $^3\text{H}$ -labeled space

marker (usually D-mannitol), one should first be certain that the two different isotopes, which also label two different molecules, do behave similarly in terms of the water space occupied by the two molecules. In other words, one should first check for the absence of any preferential binding on the filters of one isotope over the other. Since we were planning to apply the FSRFA in evaluating the kinetic characteristics of D-glucose transport in human intestinal brush-border membrane vesicles (*see* accompanying paper [21]), the following series of experiments have been performed using  $^3\text{H}$ -D-mannitol and  $^{14}\text{C}$ -D-glucose.

In the absence of vesicles, the incubation chamber was loaded with either  $^3\text{H}$ -D-mannitol ( $1.6\ \mu\text{M}$ ,  $1.5\ \mu\text{Ci}/50\text{-}\mu\text{l}$  sample) or  $^{14}\text{C}$ -D-glucose ( $46.4\ \mu\text{M}$ ,  $0.6\ \mu\text{Ci}/50\mu\text{l}$  sample), and a sequence of 18 samplings was performed. In the first run, filtration only was allowed while in the next runs, an equal but increasing number of extra washings and filtrations was performed (from one to five). The results of this experiment are shown in the second and third columns of the Table. For comparison purposes between the retentions of the two isotopes on the filters, the values have been expressed as  $\text{pmol} \cdot \text{mM}^{-1}$  from a  $50\text{-}\mu\text{l}$  aliquot. It is readily apparent from these values that both isotopes and molecules behave similarly. Moreover, in spite of a slightly decreased retention of isotopes after two washings as compared to only one, there was in fact no significant difference in filter retention between the one and five washing situations.

The same experimental protocol was repeated in the presence of 10 mM unlabeled mannitol (Table, columns 4 and 5), and the background for the two isotopes was found to be essentially identical to that observed in the first experiment. Actually, the background was even slightly increased over that of the pure isotope situation, a result which can be tentatively attributed to the viscosity change in the solutions. In any case, this experiment demonstrates the absence of any specific binding of  $^3\text{H}$ -D-mannitol to the filters as well as the insensitivity of the background in tracer D-glucose concentrations to the presence of high concentrations of D-mannitol. A stable background for both isotopes after a cycle of two washings and filtrations is obtained.

Finally, the same experimental protocol was used again in the presence of freshly prepared human brush-border membrane vesicles to test for any interaction between the space marker and the membranes. In this case, both tracer and 10-mM concentrations of  $^3\text{H}$ -D-mannitol were tested (D-glucose was not used in this experiment for obvious reasons since any uptake component might have shown up). As is apparent from the Table by comparing the last two columns with the fourth one, the presence of

**Table 1.** Binding of  $^3\text{H}$  and  $^{14}\text{C}$  isotopes on both filters and vesicles

Washings	Without vesicles				With vesicles	
	$^3\text{H}$ -D-mannitol	$^{14}\text{C}$ -D-glucose	10 mM Unlabeled mannitol		$^3\text{H}$ -D-mannitol	10 mM Unlabeled mannitol $^3\text{H}$ -D-mannitol
			$^3\text{H}$ -D-mannitol	$^{14}\text{C}$ -D-glucose		
0	243.0 $\pm$ 60.5 <sup>a</sup>	288.8 $\pm$ 79.4	304.4 $\pm$ 76.2	269.5 $\pm$ 82.8	274.4 $\pm$ 71.2	229.2 $\pm$ 71.6
1	9.7 $\pm$ 5.4 (4.0%) <sup>b</sup>	8.6 $\pm$ 5.6 (3.0%)	12.9 $\pm$ 5.9 (4.2%)	14.1 $\pm$ 5.5 (5.2%)	13.8 $\pm$ 5.6 (5.0%)	14.0 $\pm$ 6.1 (6.1%)
2	2.6 $\pm$ 1.8 (1.1%)	2.1 $\pm$ 1.9 (0.7%)	5.4 $\pm$ 3.7 (1.8%)	6.0 $\pm$ 2.3 (2.2%)	5.2 $\pm$ 3.6 (1.9%)	6.0 $\pm$ 5.4 (2.6%)
3	2.5 $\pm$ 2.1 (1.0%)	2.9 $\pm$ 2.6 (1.0%)	4.4 $\pm$ 2.4 (1.4%)	5.8 $\pm$ 2.3 (2.2%)	4.3 $\pm$ 2.4 (1.6%)	7.0 $\pm$ 3.7 (3.1%)
4	3.8 $\pm$ 2.4 (1.6%)	2.3 $\pm$ 2.1 (0.8%)	5.1 $\pm$ 2.5 (1.7%)	6.1 $\pm$ 1.9 (2.3%)	5.1 $\pm$ 2.5 (1.9%)	5.4 $\pm$ 3.8 (2.4%)
5	3.0 $\pm$ 2.2 (1.2%)	2.3 $\pm$ 2.2 (0.8%)	2.7 $\pm$ 2.0 (0.9%)	6.0 $\pm$ 2.4 (2.2%)	2.8 $\pm$ 2.0 (1.0%)	4.7 $\pm$ 2.9 (2.1%)

<sup>a</sup> Mean  $\pm$  SD from 18 determinations. Results are expressed as pmol  $\cdot$  mm<sup>-1</sup>.

<sup>b</sup> Percentage of residual substrate.

vesicles did not modify the background of D-mannitol at either concentration of the space marker. These results demonstrate the absence of any specific binding of  $^3\text{H}$ -D-mannitol on the brush-border membrane vesicles and again confirm that a stable background is achieved after a cycle of only two extra washes and filtrations.

These series of experiments thus also justify the routine procedure of one filtration plus two washings and filtrations which was adopted in all other experiments with vesicles since this procedure essentially removes 98 to 99% of the two isotopes.

## 2. Control of the Filtration Rates and Efficiency of the Stop Solution

In order to diminish as much as possible the weight of the manifold array, and thus the inertia of this moving part of the apparatus, we have chosen to construct this unit under the most compact form, and thus to use filters of 12.5-mm diameter instead of the 25-mm ones classically used in the manual application of the rapid filtration technique [15]. However, it is well known that two major limitations of the rapid filtration technique are: (i) the substrate efflux from the vesicles during the washing and filtering steps [29] which thus require a procedure as fast as possible; and (ii) the possible clogging of the filters with too high loads of vesicles [18], which will also limit the time required for filtration and washings. Obviously, both of these potential problems are minimized when using a higher surface of filtration, and a few tests were thus performed in our system to evaluate them.

In order to reduce to a minimum the duration of the filtration/washing step, we have tried filters of different porosity (0.45- and 0.65- $\mu\text{m}$  pore size) from different sources (Millipore, Sartorius, and Micro Filtration System (MFS)). In the presence of vesicles, the total duration of a cycle of one filtration followed by two washings and extra filtrations can be completed in 12 sec with the 0.65- $\mu\text{m}$  filters, a value which is significantly lower than the 18 sec obtained with the 0.45- $\mu\text{m}$  ones. No major difference in filtration performance was found between the different brands of filters. The MFS filters, however, were found to be less rigid and less expensive, and thus were chosen as preferable for routine use. Also, since the bigger pore size filters might allow for more vesicles to pass through, we next measured the initial rates of D-glucose uptake at a 50- $\mu\text{M}$  concentration in adult human jejunal brush-border membrane vesicles using MFS filters of the two porosities. The values  $\pm$  SD of regression were  $0.049 \pm 0.002$  ( $n = 8$ ) and  $0.048 \pm 0.006$  ( $n = 9$ ) nmol  $\cdot$  sec<sup>-1</sup>  $\cdot$  mg protein<sup>-1</sup> for the 0.45- and 0.65- $\mu\text{m}$  filters, respectively, thus showing that both types of filters were equivalent in terms of vesicle retention. The 0.65- $\mu\text{m}$  pore size filters were thus adopted on a routine basis for their higher filtration rates.

The precise determination of substrate uptake into (brush-border) membrane vesicles, while dependent on the time required to complete the filtration and washing step, also rely for this same reason on the ability of the stop solution to prevent any further uptake or efflux of labeled substrate from the vesicles during this step [29]. The efficiency of the stopping procedure with the FSRFA was evaluated

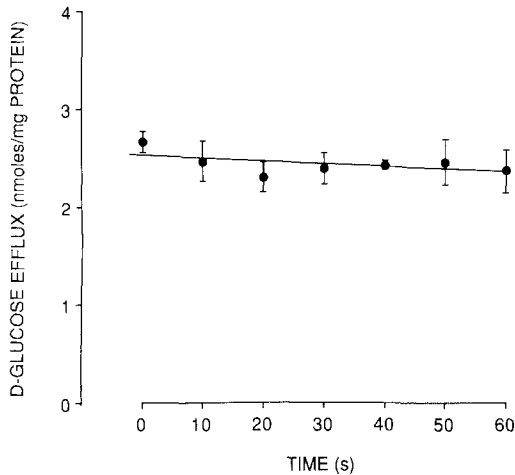


**Fig. 7.** Efficiency of the stop solution. Human jejunal brush-border membrane vesicles were resuspended in 50 mM Tris-HEPES buffer (pH 7.5), 0.1 mM  $\text{MgSO}_4$ , 100 mM KCl, 200 mM choline chloride, 10 mM mannitol and 5  $\mu\text{M}$  valinomycin. Final concentrations in the incubation media were: 50 mM Tris-HEPES buffer (pH 7.5), 0.1 mM  $\text{MgSO}_4$ , 100 mM KCl, 192 mM NaCl, 8 mM choline chloride, 10 mM mannitol, 0.5 mM amiloride, 50  $\mu\text{M}$  D-glucose,  $^3\text{H}$ -D-glucose (60  $\mu\text{Ci}/\text{ml}$ ), and  $^{14}\text{C}$ -D-mannitol (27  $\mu\text{Ci}/\text{ml}$ ). Active loading of vesicles was performed under  $\text{Na}^+$ -gradient conditions for 56 sec. Then, aliquots were collected at 0.5-sec intervals and poured into isotonic and isosmolar ice-cold stop solution containing 1 mM phlorizin and 200 mM NaCl. The filtration and washings of the samples have been done after different delay periods. Points are the means  $\pm$  SD from three determinations. Linear-regression analysis of the data points gave a y intercept of  $2.59 \pm 0.06$  nmol  $\cdot$  mg protein $^{-1}$  and a slope of  $-4.20 \cdot 10^{-3} \pm 1.71 \cdot 10^{-3}$  nmol  $\cdot$  sec $^{-1}$   $\cdot$  mg protein $^{-1}$ .

by following the time course of glucose efflux from actively loaded human intestinal brush-border membrane vesicles into the stop solution. The vesicles were loaded with D-glucose under  $\text{Na}^+$ -gradient conditions during 56 sec, a time which corresponds to the peak of the overshoot in glucose accumulation (*see* Fig. 8 below). Then, 7 aliquots were sampled at 0.5-sec intervals (mean sampling time of  $58.25 \pm 1.5$  sec) and recuperated into the manifold array, the upper chamber containing 1 ml of isotonic and isosmolar ice-cold stop solution with 1 mM phlorizin and 200 mM NaCl. The sequence of filtrations and washings of the samples was then initiated either immediately or following a delay period of increasing length, as indicated in Fig. 7. As estimated by one-way analysis of variance, there was no significant differences in the uptake values for at least the 60 sec following the dilution of the vesicles into the stop solution. However, using linear regression, the data are compatible with a loss in the vesicle content representing  $0.25$  nmol  $\cdot$  min $^{-1}$   $\cdot$  mg protein $^{-1}$ , a quantity which represents a 10% decrease over a 1-min time interval. Since the conditions chosen for

this experiment maximize the gradient in tracer concentration from inside to outside which constitutes the main driving force for efflux under these conditions, it can be calculated from the regression line that a maximum of  $0.05$  nmol  $\cdot$  mg protein $^{-1}$  (representing 1.9% of the zero time uptake value) would be lost during the 12-sec interval necessary for the routine sequence of filtration and washings with the FSRFA.

### 3. Comparison between the Manual and Fully Automatized Rapid Filtration Techniques

Figure 8 shows the 10-min time course of 50  $\mu\text{M}$   $^{14}\text{C}$ -D-glucose uptake into human intestinal brush-border membrane vesicles using either the manual rapid filtration technique or its fully automated version as allowed by the FSRFA. It clearly appears from Fig. 8 that similar uptake-time courses are obtained by the two techniques when measuring transport under  $\text{Na}^+$ -gradient conditions in the presence or absence of phlorizin. The data of Fig. 8 also shows that D-glucose uptake in adult human jejunal brush-border membrane vesicles is a transient,  $\text{Na}^+$ -dependent and phlorizin-sensitive phenomenon, thus confirming previous studies using the same preparation [6, 14, 19]. It can also be noted from Fig. 8 that the peak of the overshoot in  $\text{Na}^+$  D-glucose cotransport appears around 1 min under the conditions of this experiment.

A small difference in the protocols used for comparing the manual and the FSRFA approaches deserves some comment. As is usually done for the manual application of the technique [15], the radiolabeled space marker  $^3\text{H}$ -D-mannitol was added to the stop solution in the case of the manual uptake. However, in order to avoid contamination by radiotracer in the washing circuit of the manifold array, the vesicles were coincubated with both the space marker and the radioactive substrate in the incubation chamber when working with the FSRFA. Since the space-corrected D-glucose uptake values were found to be identical with the two techniques, one has to infer that D-mannitol does not significantly enter into the vesicles, at least over the 10-min time interval studied. This point has been evaluated directly by plotting  $^3\text{H}$ -D-mannitol uptake as a function of time. The slope of this uptake-time curve, as analyzed by linear-regression analysis, was found to represent  $2.35 \cdot 10^{-4} \pm 1.69 \cdot 10^{-4}$  pmol  $\cdot$  sec $^{-1}$  mg protein $^{-1}$ . Accordingly,  $0.141 \pm 0.101$  pmol of D-mannitol  $\cdot$  mg protein $^{-1}$  would have entered the vesicles after a 10-min incubation period, a value which represents only 0.23% of the D-glucose content measured at the same time point.

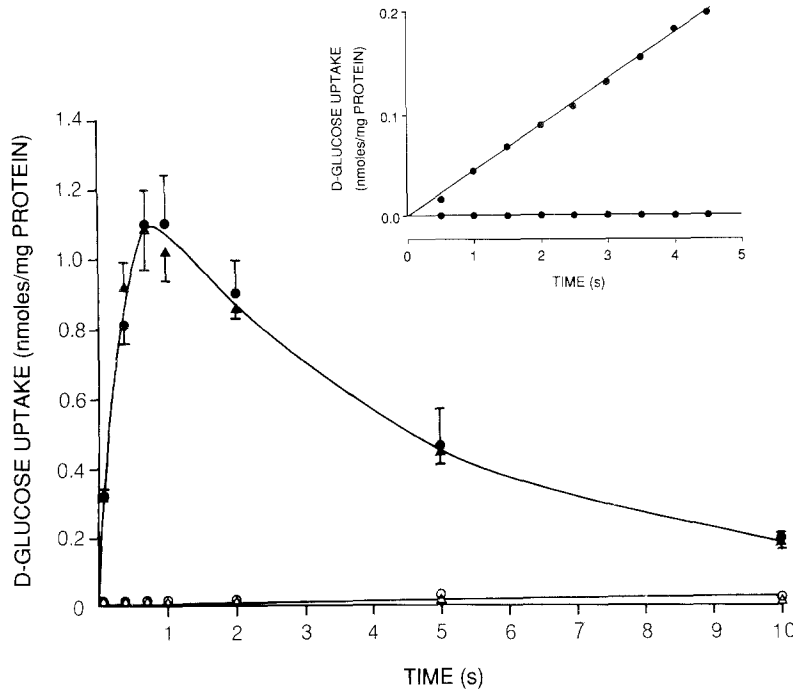


**Fig. 8.** Comparison between the manual and automated techniques. For both assays, human jejunal brush-border membrane vesicles were resuspended in 50 mM Tris-HEPES buffer (pH 7.5), 0.1 mM  $MgSO_4$ , 100 mM KCl, 200 mM choline chloride, 125 mM mannitol, and 5  $\mu M$  valinomycin. The final concentrations in the incubation media were: 50 mM Tris-HEPES buffer (pH 7.5), 0.1 mM  $MgSO_4$ , 100 mM KCl, 192 mM NaCl, 8 mM choline chloride, 125 mM mannitol, 0.5 mM amiloride, 50  $\mu M$   $^{14}C$ -D-glucose, and 1.3 mM  $^3H$ -D-mannitol.  $^3H$ -D-mannitol was added to either the stop solution or the incubation medium for the manual ( $\blacktriangle$ ,  $\triangle$ ) and automated ( $\bullet$ ,  $\circ$ ) assays, respectively. Transport was assayed under both conditions in the absence ( $\blacktriangle$ ,  $\bullet$ ) or presence ( $\triangle$ ,  $\circ$ ) of 1 mM phlorizin. Points shown are the mean  $\pm$  SD from three determinations. A typical short time uptake as obtained with the FSRFA is shown in the inset

Obviously, the results of Fig. 8 demonstrate that the FSRFA can indeed reproduce very faithfully the manual aspects of the rapid filtration technique. However, it should be noted that the FSRFA was not designed to analyze uptake-time courses over long time periods but, on the contrary, over their very early time points. Indeed, the particularly significant advantage of the FSRFA over the manual approach is clearly exemplified in the inset of Fig. 8 where nine points have been recorded over the first 4.5 sec of uptake. For comparison, it should be mentioned that our manual set up does allow for a maximum of only two time points over a time period of 5 sec from the same incubation medium. Thus, the initial rates of D-glucose uptake can be followed under real-time conditions and estimated by linear (or nonlinear, should the early time points not follow a straight line) regression analysis. For example, under the experimental conditions of Fig. 8, a linear-regression analysis of the uptake-time curve shown in the inset gave a y intercept, slope and correlation coefficient of  $-2.6 \cdot 10^{-3} \pm 2.4 \cdot 10^{-3}$  nmol  $\cdot$  mg protein $^{-1}$ ,  $0.045 \pm 0.001$  nmol  $\cdot$  sec $^{-1}$   $\cdot$  mg protein $^{-1}$  and 0.999, respectively.

#### IV. Discussion

The advantages and limitations in the use of (brush-border) membrane vesicles to study the kinetics of solute and ion transport have been recently reviewed

[4]. A conclusion of this analysis was that the meaning of transport kinetic data are highly dependent upon the validity of the initial rate assumption since the conventional approach used in the interpretation of such data has so far relied on the steady-state derivation of kinetic equations for (co)transport models. From an experimental point of view, this means that the determination of true initial rates of transport needs to be performed. Obviously, the reliability of true initial rate determinations cannot be dissociated from the reliability of the technique used in their estimation. In this context, it clearly appears that techniques allowing for real-time data analysis will always prove superior to any other method. Since optical methods for the kinetic evaluation of most solute transport are still in their infancy (*see ref. [4] for review*), thus precluding the use of stopped-flow techniques and equipment, one still has to rely on the successful application of tracer flux measurements which are most easily performed using the rapid filtration technique [15, 29]. As discussed in the introduction, the application of this technique involves basically three steps and, as such, makes difficult its application to real-time data analysis. To our knowledge, such an approach has so far not yet been attempted in the field of transport, and it was thus the main goal of our studies to develop such a technique. These studies were also prompted by the recent demonstration that nonlinear initial rate kinetics might be observed in particu-

lar transport systems [3, 24], in accordance with the expectations from theoretical considerations as to the occurrence of presteady-state kinetics in (co)-transport systems [24, 30].

The FSRFA, which we describe in this paper, thus appears to fill a gap in the techniques currently available for transport measurements by allowing for real-time studies. Indeed, the FSRFA reproduces accurately the manual version of the rapid filtration technique while improving initial rate determinations through multiple sampling from the same incubation mixture over very short time intervals. Moreover, the dead time of the FSRFA, which is almost entirely determined by the sampling process and linearly related to the sampling volume, compares fairly well with the one time point apparatus of Kessler et al. [16]. It can be easily appreciated that, under the conditions used in the initial rate determination of the transport experiment described in the inset of Fig. 8, the dead time of the FSRFA only represents 5% variation around the mean-time value of the first sampling time and decreases very rapidly thereafter. The FSRFA has also been designed to provide as much versatility as possible. For example, in its actual version, it provides a very precise control of the incubation temperature and should permit an accurate determination of temperature effects on transport phenomena. Moreover, a few efflux studies can be performed, even though the FSRFA has not yet addressed the main problems of such studies (*see* ref. [4] for review). Modifications from the basic set up should however allow for a control of some of these and are currently considered in our laboratory. For influx studies on the other hand, the FSRFA has addressed and solved most if not all of the problems which are inherent to the rapid filtration technique. Under these experimental conditions, the FSRFA permits use of a dynamic approach in the evaluation of transport kinetics which, as compared to the one time point estimation of initial rates, clearly presents the following advantages [4]: (i) determination of true initial rate under all of the conditions of a kinetic experiment; (ii) possible discrimination between the different processes contributing to total uptake; and (iii) easy determination of the standard error of measurement (and thus of a weighting factor) for each rate contributing to the final analysis of the data according to model equations. Some of these advantages appear more clearly in the accompanying paper [21].

Although the FSRFA has primarily been designed for application to transport flux measurements in (brush-border) membrane vesicles, it should, however, be stressed that this apparatus is of much broader interest since it is perfectly suited to any radiotracer study or enzyme reactions that

needed to be terminated by a filtration step. As such, it could be very helpful to biochemists, physiologists and pharmacologists involved in binding/receptor studies and/or kinetic determinations of phosphorylation reactions. Also, with just a few minor modifications, the apparatus should be easily adaptable to recuperate the filtrate during the filtration step. Finally, the clear separation between the fast sampling module (represented by the incubation chamber and its functioning circuits) and the rapid filtration device should also allow for more applications. For example, in our laboratory, we have recently been able to measure both the kinetics of glucose-6-phosphate hydrolysis by rat hepatic microsomes and the consecutive product accumulation into the microsomal vesicles and, for the first time, to demonstrate a hysteretic behavior of the enzyme [5]. While the second part could be performed using a set up similar to the one described in the present paper, the first one was easily performed after disconnection of the rapid filtration unit and introducing into the upper chamber of the manifold array 18 small centrifuge tubes, each containing a quenched stop solution in order to recuperate and stop the reaction in the different samples [5]. As such, the FSRFA could also constitute an alternative to the current use of quenched-flow machines, at least for transient reactions occurring in the time range of a few seconds. It is quite clear, however, that the latter will always prove superior to the FSRFA in terms of dead time, accuracy, and accessible time ranges, while not allowing for multiple sampling from the same incubation mixture.

We are currently investigating the possibility of having the FSRFA produced on a commercial basis. To anyone interested in developing such a machine, however, it might be useful to know that the budget required for setting up the machine described herein should include approximately US \$10,000 for a microcomputer and the equipment listed in section B of Materials and Methods, and a salary for a professional corresponding to a minimum of 300 hr labor time, not including the time necessary to develop the electronic circuitry and software.

This research was supported by grants MA-8923 and MA-7607 from the Medical Research Council of Canada. C.M. and A.B. are both supported by a scholarship from the "Fonds de la Recherche en Santé du Québec." The authors thank Miss H. Collette for her secretarial help and Messrs. G. Filosi, C. Gauthier, and D. Cyr for the artwork.

## References

1. Aronson, P.S. 1981. Identifying secondary active solute transport in epithelia. *Am. J. Physiol.* **240**:F1-F11
2. Berteloot, A. 1984. Characteristics of glutamic acid transport

- by rabbit intestinal brush-border membrane vesicles. *Biochim. Biophys. Acta* **775**:129–140
3. Berteloot, A. 1986. Membrane potential dependency of glutamic acid transport in rabbit jejunal brush-border membrane vesicles:  $K^+$  and  $H^+$  effects. *Biochim. Biophys. Acta* **857**:180–188
  4. Berteloot, A., Semenza, G. 1990. Advantages and limitations of vesicles for the characterization and the kinetic analysis of transport systems. In: *Methods in Enzymology. Biomembranes. Part W. Cellular and Subcellular Transport: Epithelial Cells*. Vol. 192. pp. 409–437. S. Fleischer and B. Fleischer, editors. Academic, Orlando, FL
  5. Berteloot, A., Vidal, H., Larue, M.J., Van De Werwe, G. 1991. Rapid kinetics of liver microsomal glucose-6-phosphatase: I. Evidence for tight-coupling between glucose-6-phosphate transport and phosphohydrolase activity. *J. Biol. Chem.* (in press)
  6. Bluett, M.K., Abumrad, N.N., Arab, N., Ghishan, F.K. 1986. Aboral changes in D-glucose transport by human intestinal brush-border membrane vesicles. *Biochem. J.* **237**:229–234
  7. Busse, D. 1978. Transport of L-arginine in brush border vesicles derived from rabbit kidney cortex. *Arch. Biochem. Biophys.* **191**:551–560
  8. Champeil, P., Guillain, F. 1986. Rapid filtration study of the phosphorylation-dependent dissociation of calcium from transport sites of purified sarcoplasmic reticulum ATPase and ATP modulation of the catalytic cycle. *Biochemistry* **25**:7023–7033
  9. Dorando, F.C., Crane, R.K. 1984. Studies of the kinetics of  $Na^+$  gradient-coupled glucose transport as found in brush-border membrane vesicles from rabbit jejunum. *Biochim. Biophys. Acta* **772**:273–287
  10. Dupont, Y. 1984. A rapid-filtration technique for membrane fragments or immobilized enzymes: Measurements of substrate binding or ion fluxes with a few-millisecond time resolution. *Anal. Biochem.* **142**:504–510
  11. Forbush, B., III. 1984. An apparatus for rapid kinetics analysis of isotopic efflux from membrane vesicles and of ligand dissociation from membrane proteins. *Anal. Biochem.* **140**:495–505
  12. Gasco, O.D., Knowles, A.F., Shertzer, H.G., Suolinn, E.M., Racker, E. 1976. The use of ion-exchange resins for studying ion transport in biological systems. *Anal. Biochem.* **72**:57–65
  13. Grunhagen, H.H. 1980. Fast tracer efflux from membrane vesicles: Investigation by controlled elution. *Anal. Biochem.* **109**:18–26
  14. Harig, J.M., Barry, J.A., Rajendran, V.M., Soergel, K.H., Ramaswamy, K. 1989. D-glucose and L-leucine transport by human intestinal brush border membrane vesicles. *Am. J. Physiol.* **256**:G618–G623
  15. Hopfer, U., Nelson, K., Perrotto, J., Isselbacher, K.J. 1973. Glucose transport in isolated brush-border membrane from rat small intestine. *J. Biol. Chem.* **248**:25–32
  16. Kessler, M., Tannenbaum, V., Tannenbaum, C. 1978. A simple apparatus for performing short-time (1–2 seconds) uptake measurements in small volumes: its application to D-glucose transport studies in brush border vesicles from rabbit jejunum and ileum. *Biochim. Biophys. Acta.* **509**:348–359
  17. Kunst, A., Draeger, B., Ziegenhorn, J. 1984. UV-methods with hexokinase and glucose-6-phosphate dehydrogenase. In: *Methods of Enzymatic Analysis*. (3rd ed.) Vol. 6, pp. 163–172. Metabolites 1: Carbohydrates. H.U. Bergmeyer, editor. Verlag Chemie, Weinheim
  18. Lever, J.E. 1980. The use of membrane vesicles in transport studies. *CRC Crit. Rev. Biochem.* **7**:187–246
  19. Lucke, H., Berner, W., Menge, H., Murer, H. 1978. Sugar transport by brush border membrane vesicles isolated from human small intestine. *Pfluegers Arch.* **373**:243–248
  20. Malo, C. 1988. Kinetic evidence for heterogeneity in  $Na^+$ -D-glucose cotransport systems in the normal human fetal small intestine. *Biochim. Biophys. Acta* **938**:181–188
  21. Malo, C., Berteloot, A. 1991. Analysis of kinetic data in transport studies: New insights from kinetic studies of  $Na^+$ -D-glucose cotransport in human intestinal brush-border membrane vesicles using a fast sampling, rapid filtration apparatus. *J. Membrane Biol.* **122**:
  22. Murer, H., Biber, J., Gmaj, P., Stieger, B. 1984. Cellular mechanisms in epithelial transport: Advantages and disadvantages of studies with vesicles. *Mol. Physiol.* **6**:55–82
  23. Murer, H., Gmaj, P. 1986. Transport studies in plasma membrane vesicles isolated from renal cortex. *Kidney Int.* **30**:171–186
  24. Otsu, K., Kinsella, J., Sacktor, B., Froehlich, J.P. 1989. Transient state kinetic evidence for an oligomer in the mechanism of  $Na^+$ - $H^+$  exchange. *Proc. Natl. Acad. Sci. USA.* **86**:4818–4822
  25. Paraschos, A., Gonzales-Ros, J.M., Martinez-Carrion, M. 1983. Absorption filtration. A tool for the measurement of ion tracer flux in native membranes and reconstituted lipid vesicles. *Biochim. Biophys. Acta* **733**:223–233
  26. Schmitz, J., Preiser, H., Maestracci, D., Ghosh, B.K., Cerda, J.J., Crane, R.K. 1973. Purification of the human intestinal brush border membrane. *Biochim. Biophys. Acta* **323**:98–112
  27. Semenza, G., Kessler, M., Hosang, M., Weber, J., Schmidt, U. 1984. Biochemistry of the  $Na^+$ , D-glucose cotransporter of the small-intestinal brush-border membrane. The state of the art in 1984. *Biochim. Biophys. Acta* **779**:343–379
  28. Torrent-Quetglas, M. 1985. Oil-stop method as an alternative to filtration for transport studies on plasma membrane vesicles. A preliminary report. *Rev. Esp. Fisiol.* **41**:177–182
  29. Turner, R.J. 1983. Quantitative studies of cotransport systems: Models and vesicles. *J. Membrane Biol.* **76**:1–15
  30. Wierzbicki, W., Berteloot, A., Roy, G. 1990. Presteady-state kinetics and carrier-mediated transport: A theoretical analysis. *J. Membrane Biol.* **117**:11–27

Received 23 January 1991